Electronic Supplementary Material (ESI) for New Journal of Chemistry.
This journal is © The Royal Society of Chemistry and the Centre National de la Recherche Scientifique 2021

Supporting Information

Ln(III) complexes with a chiral 1*H*-pyrazolo[3,4-*b*]pyridine derivative fused with a (–)-*α*-pinene moiety: synthesis, crystal structure, and photophysical studies in solution and in the solid state

Yuliya A. Bryleva,[a,b,*] Yuliya P. Ustimenko,[c] Victor F. Plyusnin,[b,d] Alexsandr V. Mikheilis,[d] Aleksandr A. Shubin,[b,e] Ludmila A. Glinskaya,[a] Vladislav Yu. Komarov,[a,b] Alexander M. Agafontsev,[b,c] Alexey V. Tkachev[b,c]

[a]*Nikolaev Institute of Inorganic Chemistry, Siberian Branch of the Russian Academy of Sciences, 3, Acad. Lavrentiev Ave., Novosibirsk 630090, Russia*

[b]*Novosibirsk State University, 2, Pirogova Str., 630090 Novosibirsk, Russia*

[c]*Vorozhtsov Novosibirsk Institute of Organic Chemistry, Siberian Branch of the Russian Academy of Sciences, 9, Acad. Lavrentiev Ave., Novosibirsk 630090, Russia*

[d]*Institute of Chemical Kinetics and Combustion, Siberian Branch of the Russian Academy of Sciences, 3, Institutskaya Str., Novosibirsk 630090, Russia*

[e]*Boreskov Institute of Catalysis, Siberian Branch of the Russian Academy of Sciences, 5, Acad. Lavrentiev Ave., Novosibirsk 630090, Russia*

[*]Corresponding author at: Nikolaev Institute of Inorganic Chemistry, Siberian Branch of the Russian Academy of Sciences, 3, Academician Lavrentiev Avenue, Novosibirsk 630090, Russia.
E-mail address: bryleva@niic.nsc.ru (Yuliya A. Bryleva).

Content

Table S1 Selected bond lengths and angles for complex **2**.....3
Table S2 ESI mass spectral data for complexes **1**–**3** 4
Fig. S1 TG, DTA, and DTG of complexes **1**–**3** 5
Fig. S2 IR spectra of free L and complexes **1**−**3**. 6
Fig. S3 ^{1}H and ^{13}C NMR spectra of free ligand L.....7
Fig. S4 ^{1}H and ^{13}C NMR spectra of complex **1** 8
Fig. S5 ^{1}H NMR spectra of complexes **2** and **3**.....9
Fig. S6 Comparison of the ^{1}H NMR spectra of free ligand L and complexes **1**–**3**. 10
Fig. S7 Possible binding modes for ligand L to the Ln center in complexes **1**−**3**.....11
Fig. S8 Possible diastereomers for complexes **1**−**3**. 12
Fig. S9 Simulated XRPD pattern of complex **2** and experimental ones of complexes **1**−**3**.....13
Fig. S10 Kinetics of luminescence decay of L in MeCN and in the solid state at 300 K 14
Fig. S11 Luminescence spectra of L in the solid state and in MeCN at 77 K.....15
Fig. S12 Normalized excitation spectra of complexes **1**–**3** in MeCN at 300 K. 16
Fig. S13 Normalized excitation spectra of complexes **1**–**3** in the solid state at 300 K. 17
Fig. S14 Kinetics of luminescence decay of complex **2** in the solid state at 615 and 537 nm.....18
Fig. S15 Kinetics of luminescence decay of complex **2** in MeCN at 615 and 537 nm.....19
Fig. S16 Normalized luminescence spectrum of complex **2** in the solid state at 300 K 20
Fig. S17 Optimized structure of L within the PCM model taking into account four nearest MeCN molecules and experimental and calculated absorption spectra of L 21
Fig. S18 The experimental and calculated absorption spectra of L obtained using various functionals 22
Fig. S19 The nature of the molecular orbitals of L involved in the first five transitions ($S_0 \rightarrow S_{1,2,3,4,5}$).....23
Fig. S20 Optimized structure of L in the S_1 excited state within the PCM model 24

Table S1 Selected bond lengths and angles for complex **2**[a]

Bond	Bond lengths (Å)	Bond	Bond lengths (Å)
Eu(1)–O(4)	2.484(4)x2	C(1)–C(2)	1.508(8)
Eu(1)–O(1)	2.495(5)x2	C(1)–C(6)	1.557(10)
Eu(1)–O(2)	2.508(4)x2	C(1)–C(7)	1.561(9)
Eu(1)–N(3)	2.587(5)x2	C(2)–C(10)	1.388(9)
Eu(1)–N(1)	2.606(5)x2	C(2)–C(3)	1.421(9)
O(1)–N(5)	1.267(7)	C(3)–C(4)	1.517(9)
O(2)–N(5)	1.269(7)	C(4)–C(5)	1.523(9)
O(3)–N(5)	1.223(8)	C(5)–C(7)	1.547(9)
O(4)–N(6)	1.282(5)	C(5)–C(6)	1.569(9)
O(6)–N(6)	1.216(8)	C(6)–C(9)	1.514(9)
N(1)–N(2)	1.386(7)	C(6)–C(8)	1.530(9)
N(1)–C(13)	1.322(8)	C(10)–C(11)	1.397(9)
N(2)–C(12)	1.385(7)	C(11)–C(12)	1.403(9)
N(2)–C(15)	1.412(8)	C(11)–C(13)	1.418(10)
N(3)–C(15)	1.337(7)	C(13)–C(14)	1.486(12)
N(3)–C(19)	1.338(7)	C(15)–C(16)	1.387(9)
N(4)–C(12)	1.334(8)	C(16)–C(17)	1.383(9)
N(4)–C(3)	1.348(8)	C(17)–C(18)	1.377(8)
N(6)–O(4)'	1.282(5)	C(18)–C(19)	1.376(9)
N(7)–C(20)	1.13(2)	C(20)–C(21)	1.40(2)
Angle	Angle size (º)	Angle	Angle size (º)
N(1)–Eu(1)–N(3)	61.8(2)	O(4)–Eu(1)–O(4)'	52.1(2)
O(1)–Eu(1)–O(2)	51.3(2)	O(1)–Eu(1)–O(1)'	140.6(3)
N(1)–Eu(1)– N(1)'	72.1(2)	O(2)–Eu(1)–O(2)'	179.5(2)
N(3)–Eu(1)–N(3)'	160.2(2)		

[a]Symmetry transformation used to generate equivalent atoms: ' = 1−x, 1−y, z.

Table S2 ESI mass spectral data for complexes **1**–**3**

Ion	Ln = Sm (**1**)		Ln = Eu (**2**)		Ln = Tb (**3**)	
	$m/z_{measured}$	$m/z_{calculated}$	$m/z_{measured}$	$m/z_{calculated}$	$m/z_{measured}$	$m/z_{calculated}$
$[LnL_2(NO_3)_2]^+$	884.25	884.23	885.25	885.23	891.25	891.24
$[LnL(NO_3)_2]^+$	580.05	580.06	581.05	581.07	587.05	587.07
$[Ln_2L_3(NO_3)_5]^+$	1526.45	1526.28	1528.34	1528.28	1540.31	1540.29
$[LnL_3(NO_3)_3 + K^+]$	–	–	986.20	986.19	–	–
$[LnL_3(NO_3)_3 + H^+]$	–	–	948.25	948.23	954.25	954.23

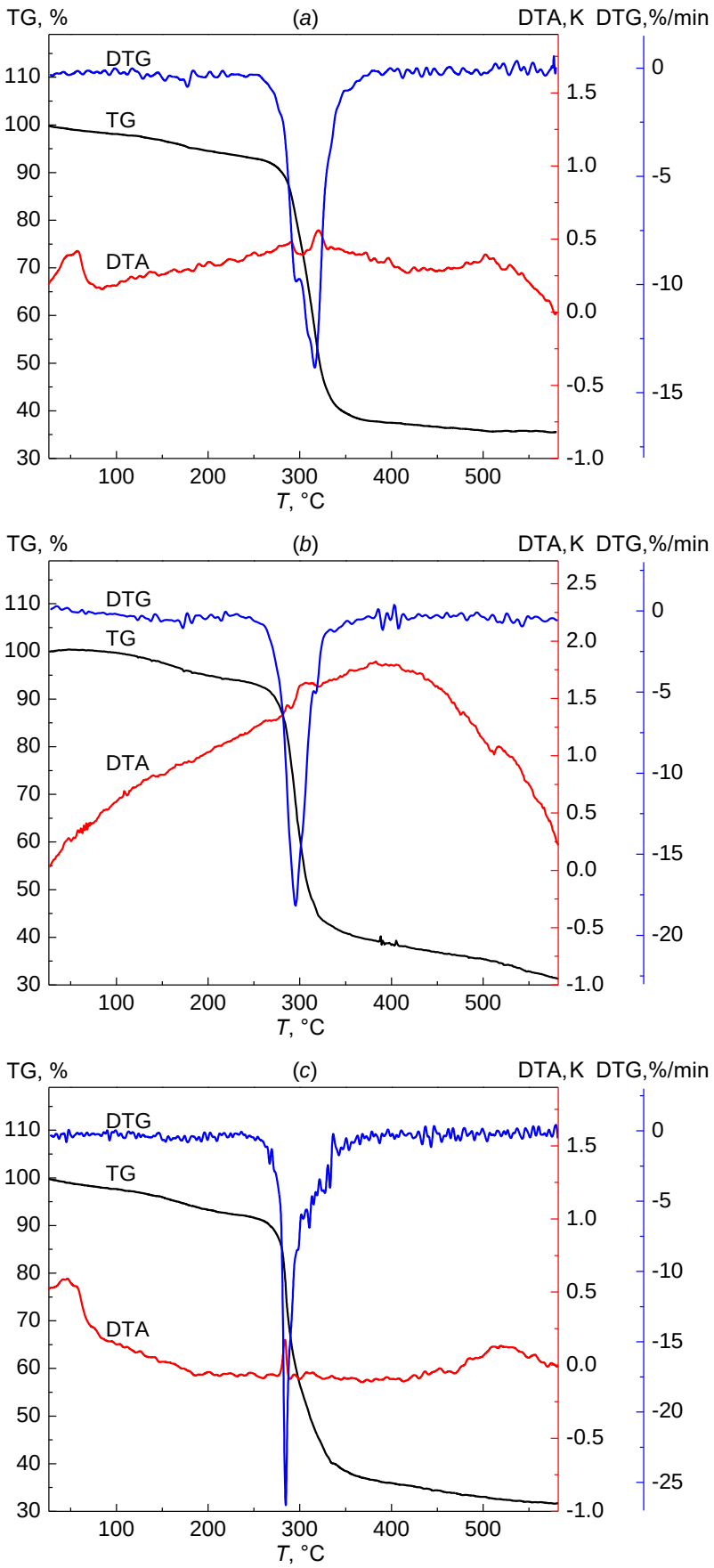

Fig. S1 TG, DTA, and DTG of complexes **1** (*a*), **2** (*b*) and **3** (*c*).

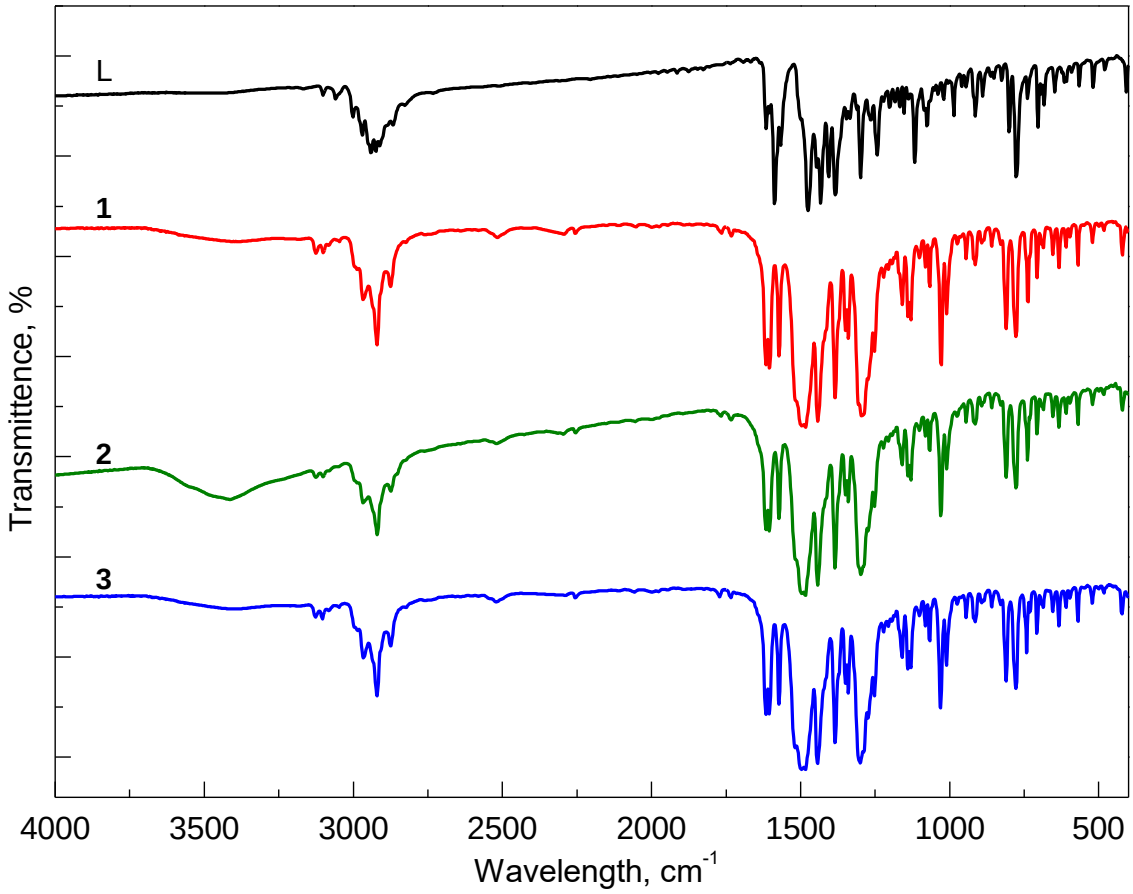

Fig. S2 IR spectra of free L and complexes **1**–**3**.

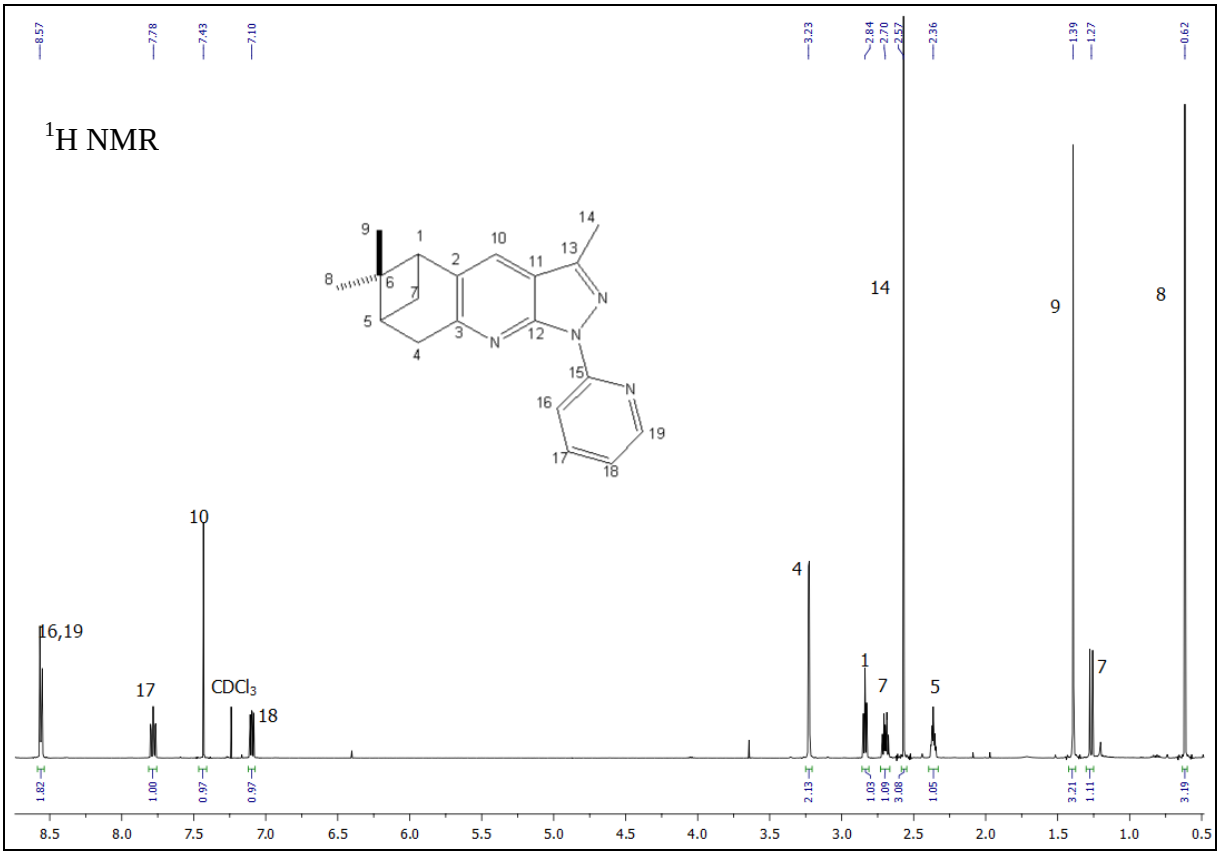

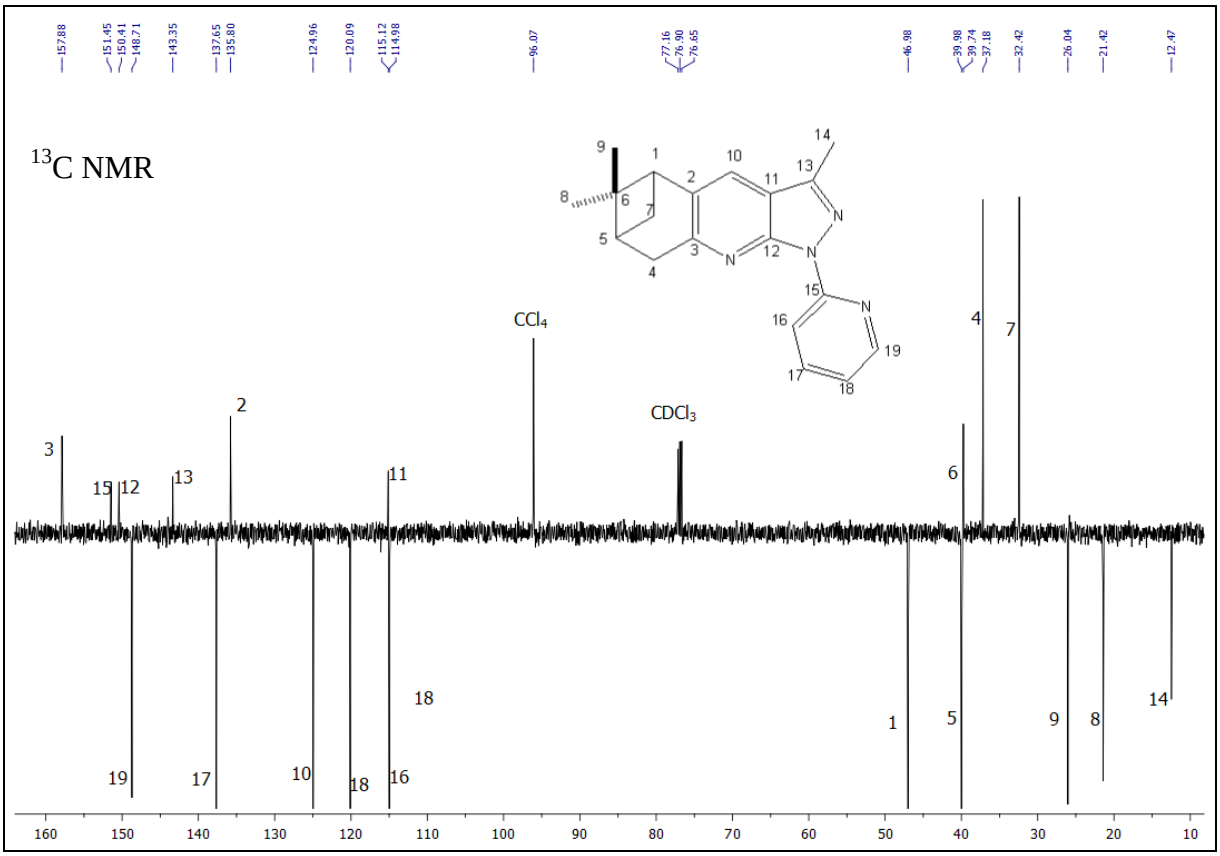

Fig. S3 ^{1}H and ^{13}C NMR spectra of free ligand L.

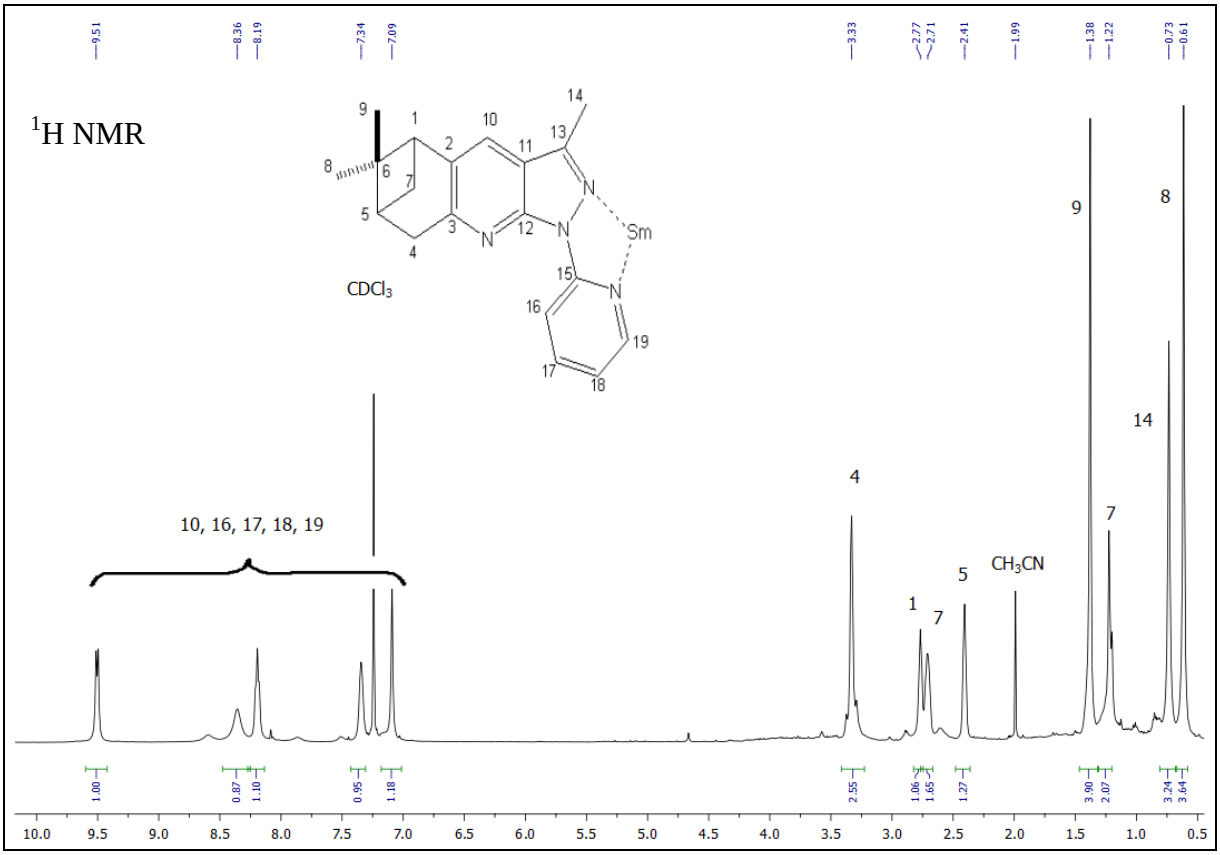

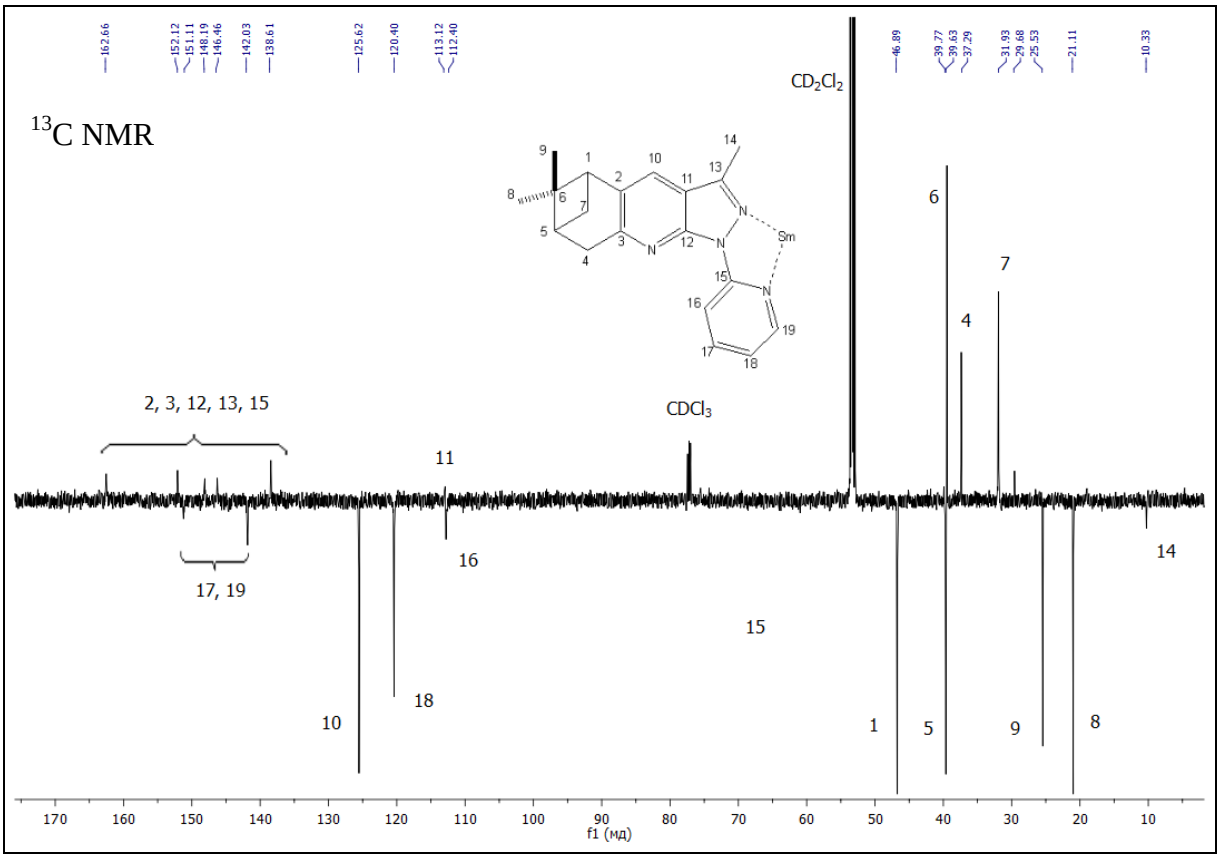

Fig. S4 ^{1}H and ^{13}C NMR spectra of complex **1**.

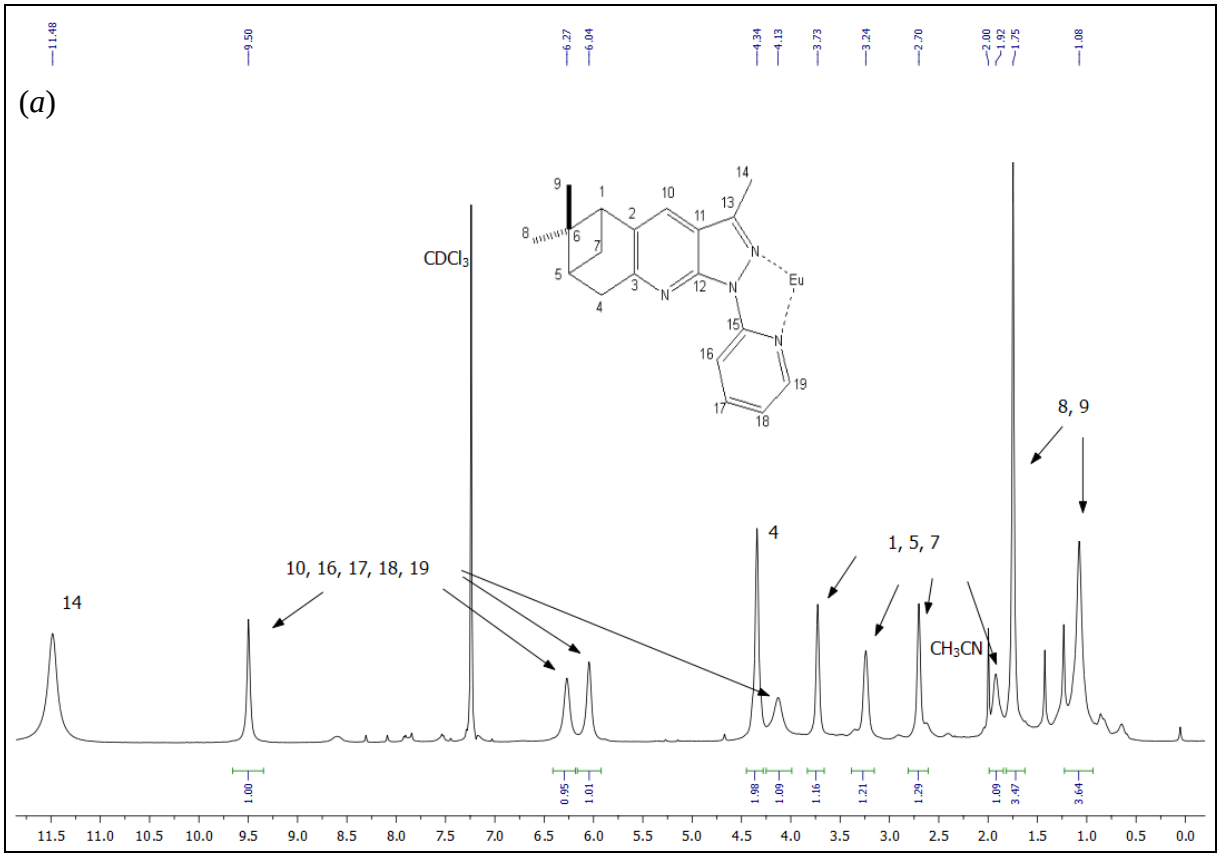

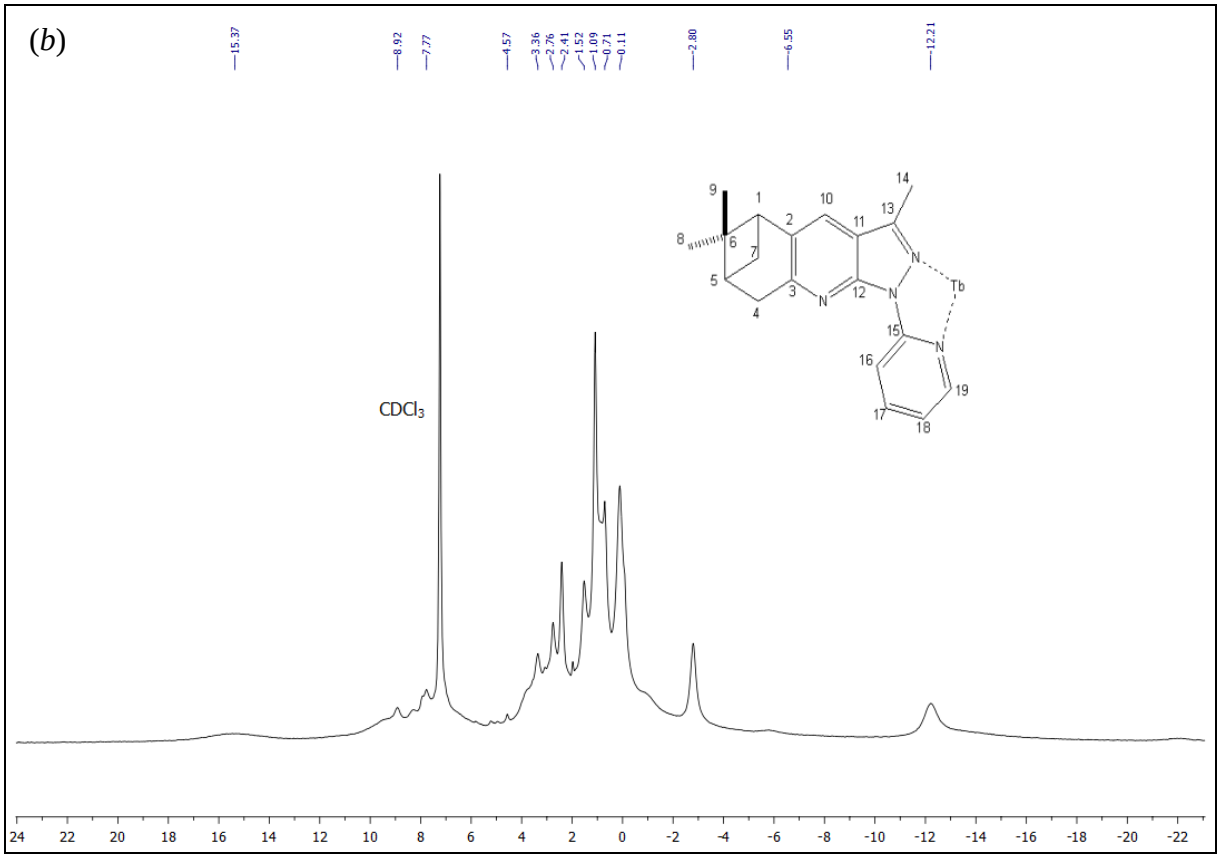

Fig. S5 ^{1}H NMR spectra of complexes **2** (*a*) and **3** (*b*).

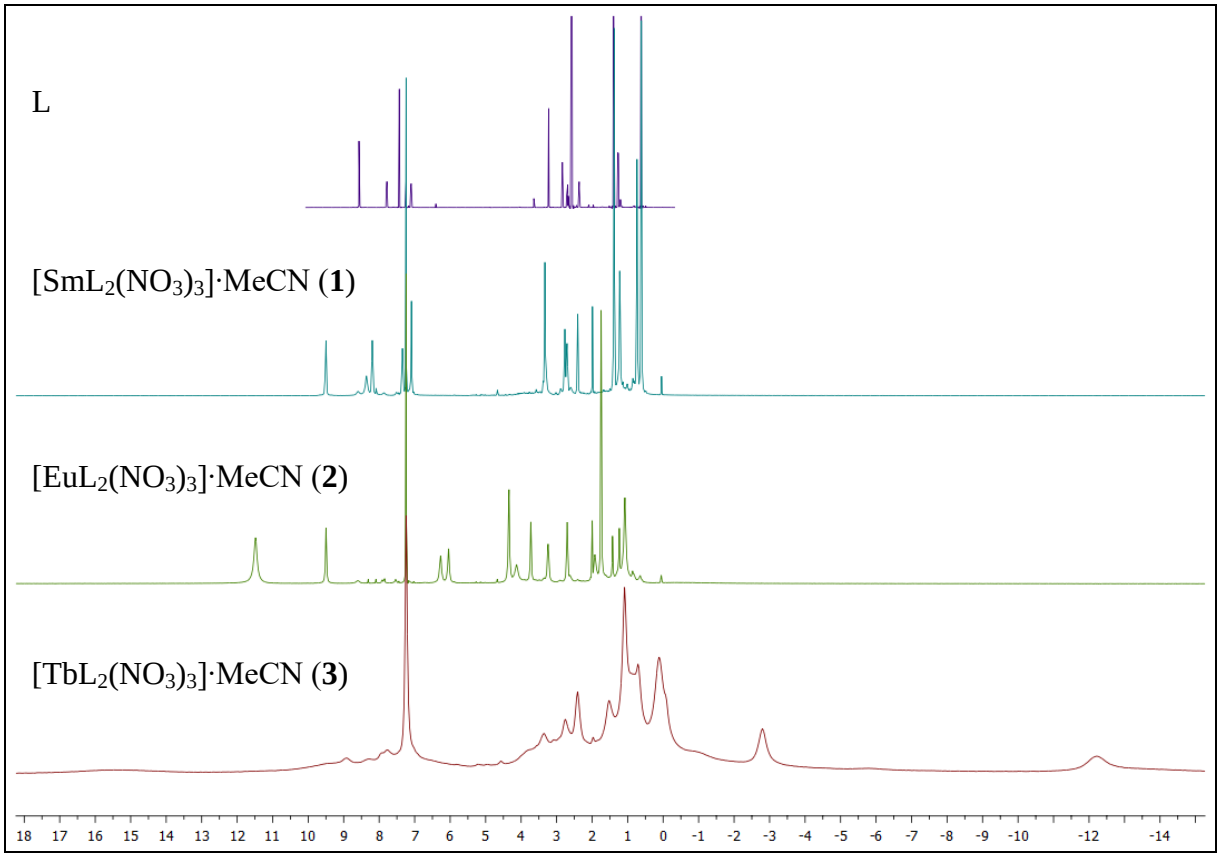

Fig. S6 Comparison of ^{1}H NMR spectra of free ligand L and complexes **1**–**3**.

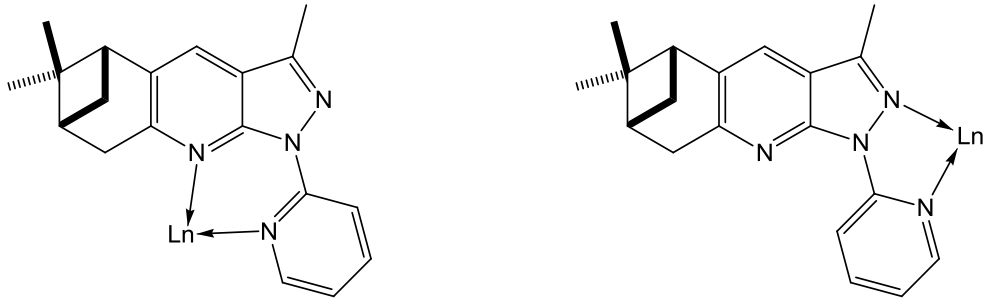

(*i*) (*ii*)

Fig. S7 Possible binding modes for ligand L to the Ln center in complexes **1**−**3**.

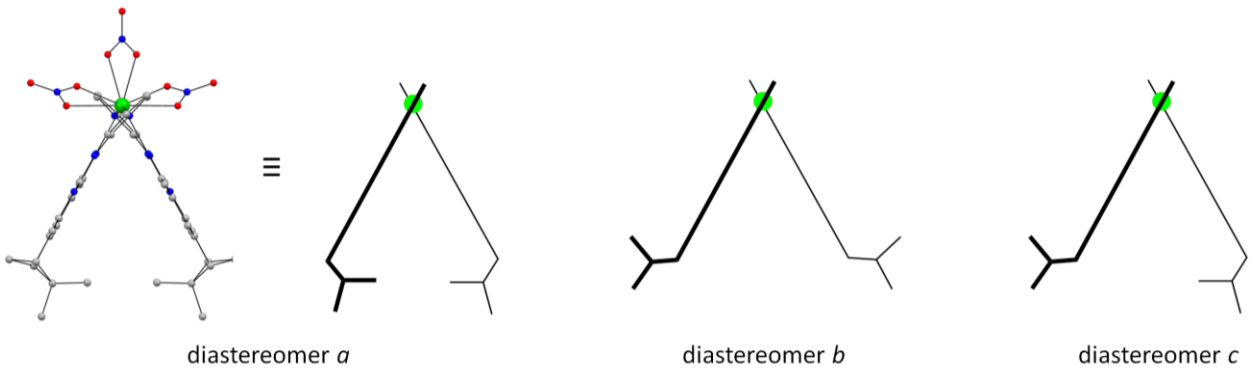

Fig. S8 Possible diastereomers for complexes **1**−**3**.

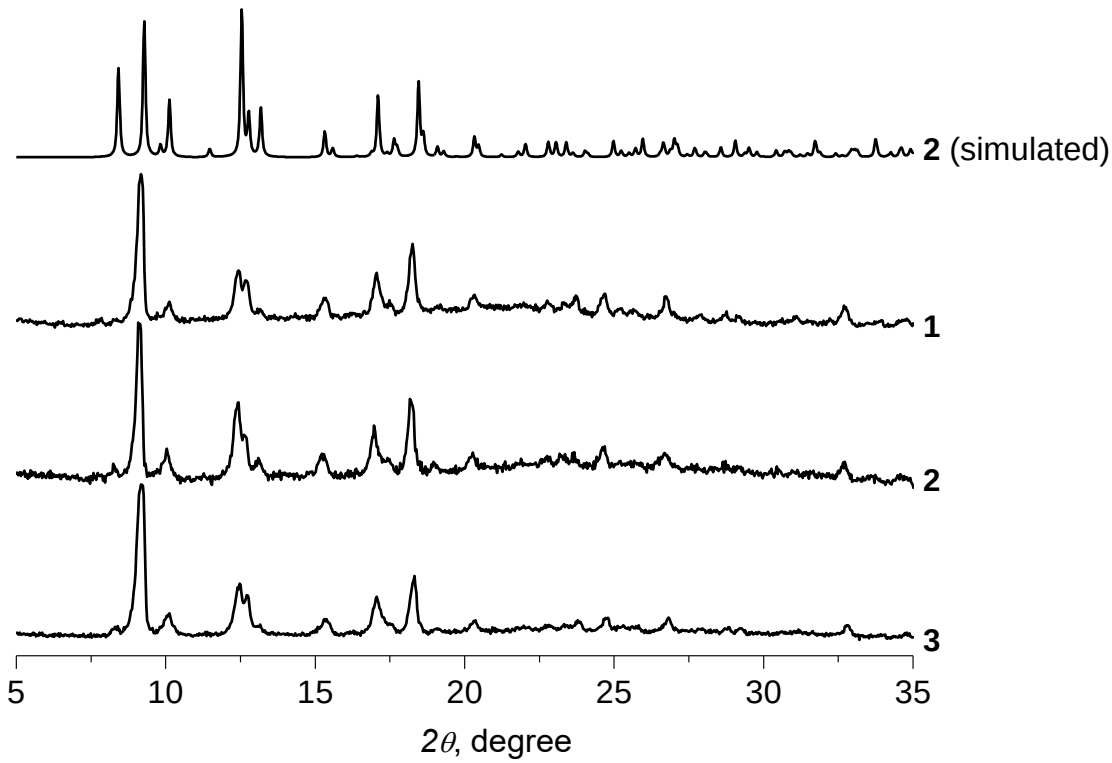

Fig. S9 Simulated XRPD pattern of complex **2** and experimental ones of complexes **1**–**3**

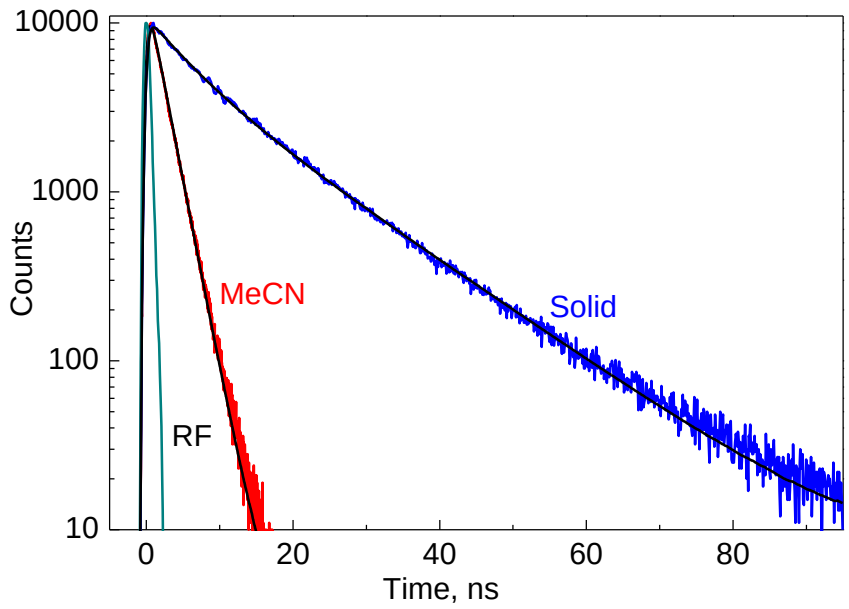

Fig. S10 Kinetics of luminescence decay of L at 360 nm in MeCN and in the solid state at 300 K. Excitation at 300 nm. The solid lines are calculated curves with the parameters listed in Table 2. RF is response function.

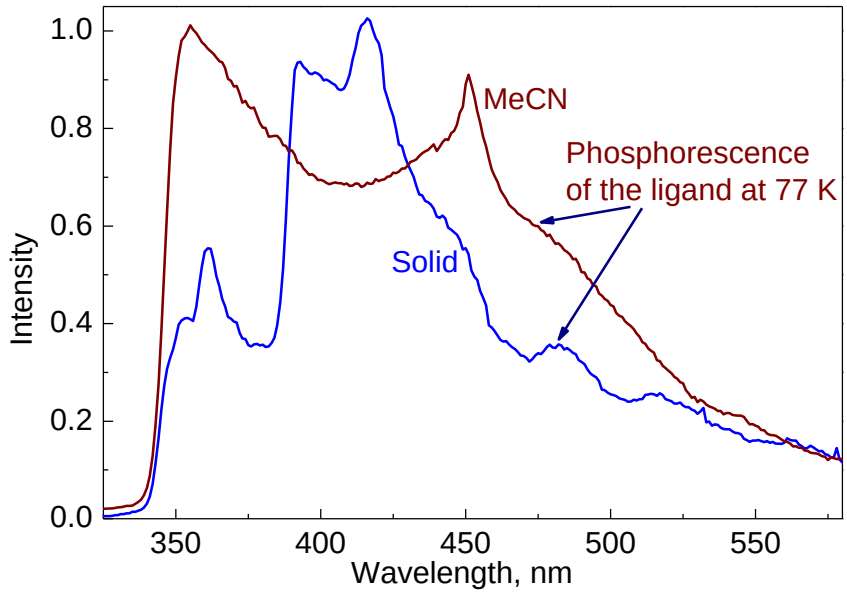

Fig. S11 Luminescence spectra of L in the solid state and in MeCN at 77 K. The arrows indicate the positions of the phosphorescence bands.

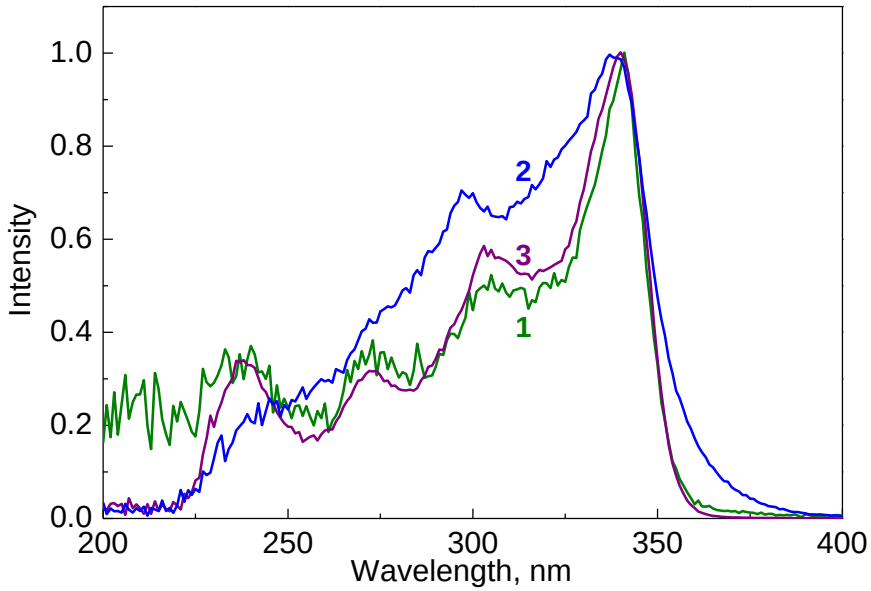

Fig. S12 Normalized excitation spectra of complexes **1** (luminescence at 644 nm), **2** (615 nm), and **3** (545 nm) in MeCN at 300 K.

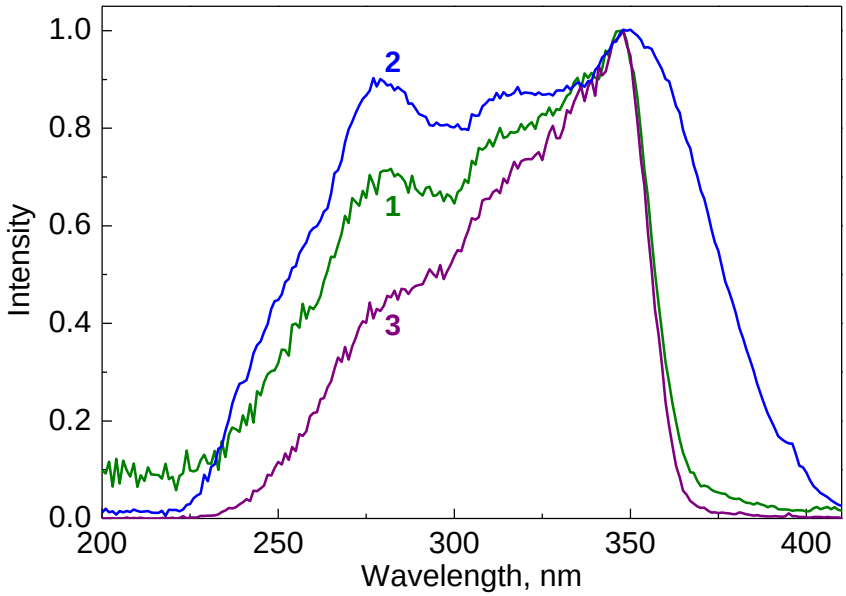

Fig. S13 Normalized excitation spectra of complexes **1** (luminescence at 644 nm), **2** (615 nm), and **3** (545 nm) in the solid state at 300 K.

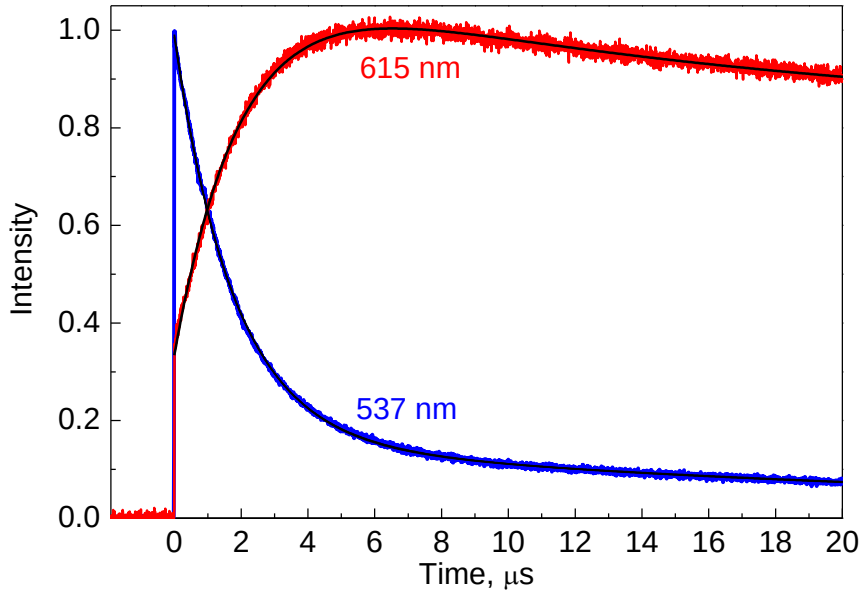

Fig. S14 Kinetics of luminescence decay of complex **2** in the solid state at 615 and 537 nm at 300 K. Excitation at 266 nm. The solid lines are calculated curves with the parameters listed in Table 2.

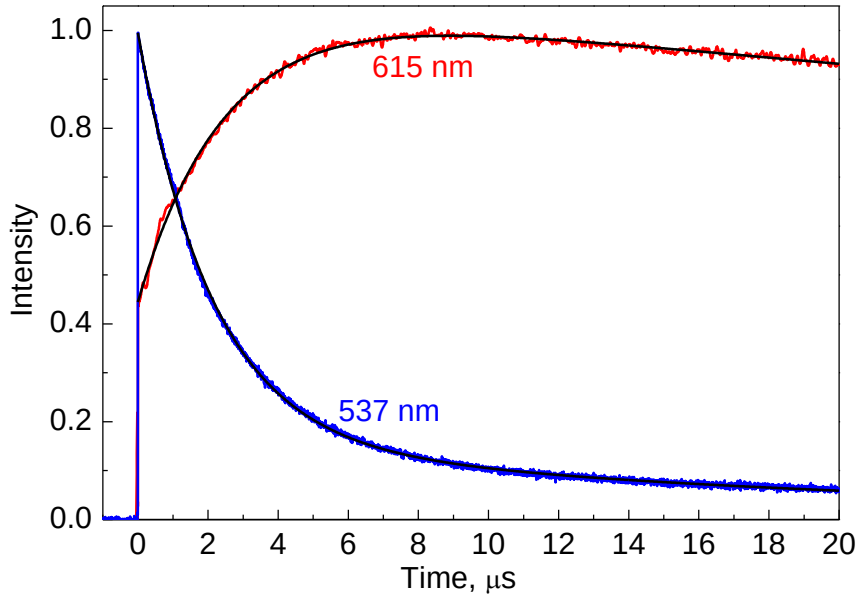

Fig. S15 Kinetics of luminescence decay of complex **2** in MeCN at 615 and 537 nm at 300 K. Excitation at 266 nm. The solid lines are calculated curves with the parameters listed in Table 2.

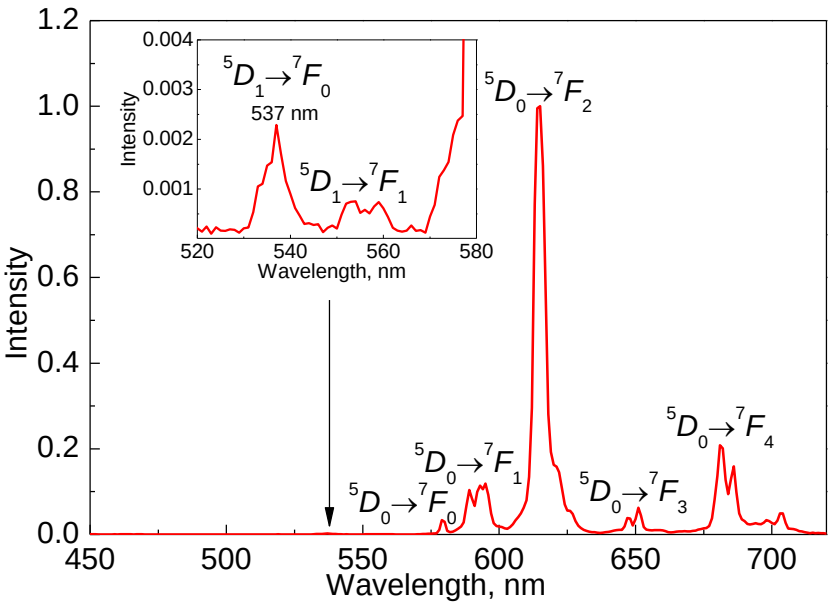

Fig. S16 Normalized luminescence spectrum of complex **2** in the solid state at 300 K. Inset shows an enlarged part of the spectrum with the $^5D_1 \rightarrow {}^7F_0$ transition at 537 nm. Excitation at 300 nm.

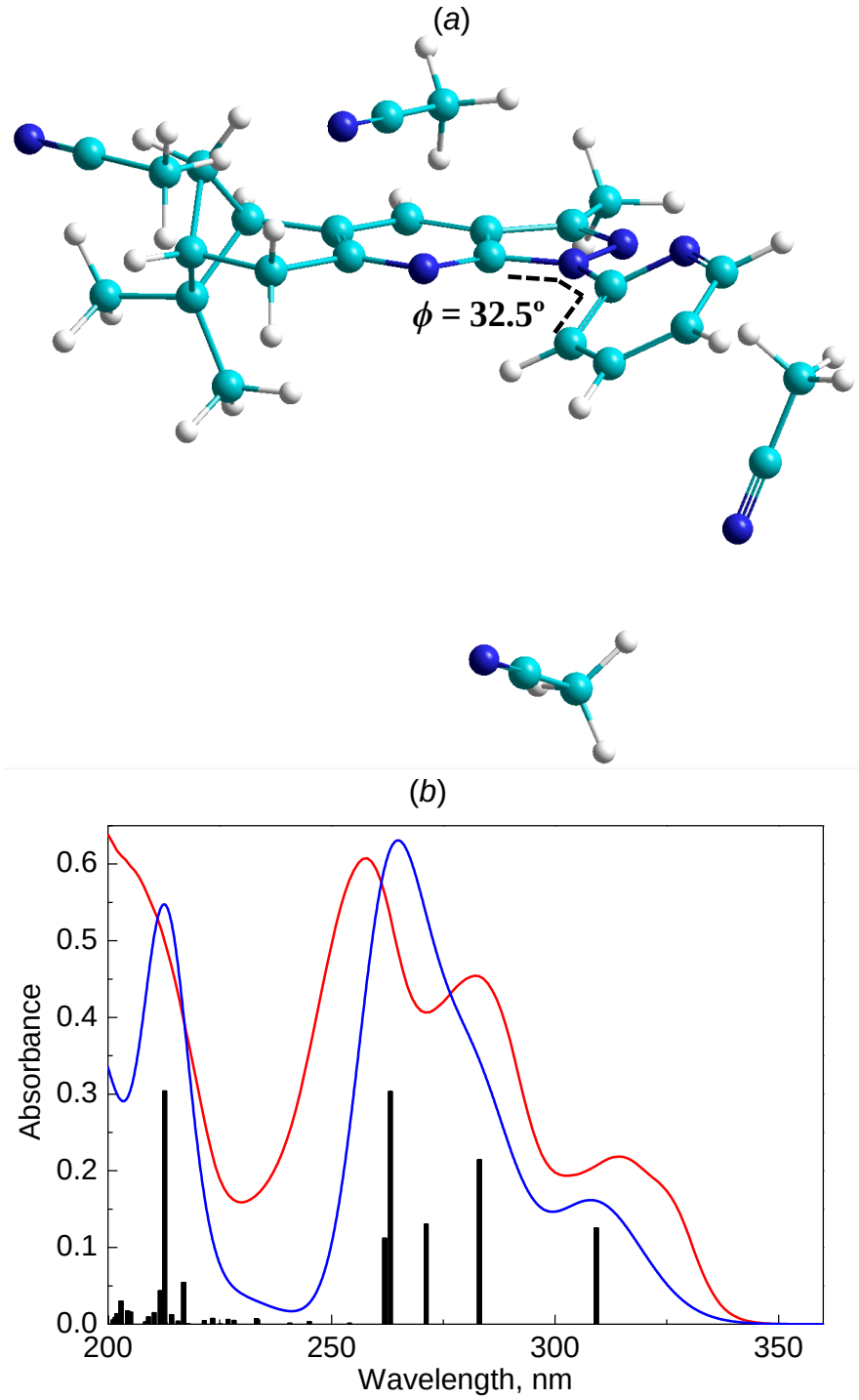

Fig. S17 (*a*) Optimized structure of L within the PCM model taking into account four nearest MeCN molecules. The C−N−C−C torsion angle is the angle between the averaged planes of 5- and 6-membered rings. (*b*) Experimental (red) and calculated (blue) absorption spectra of L. Vertical lines are the energies and the oscillator strengths of transitions.

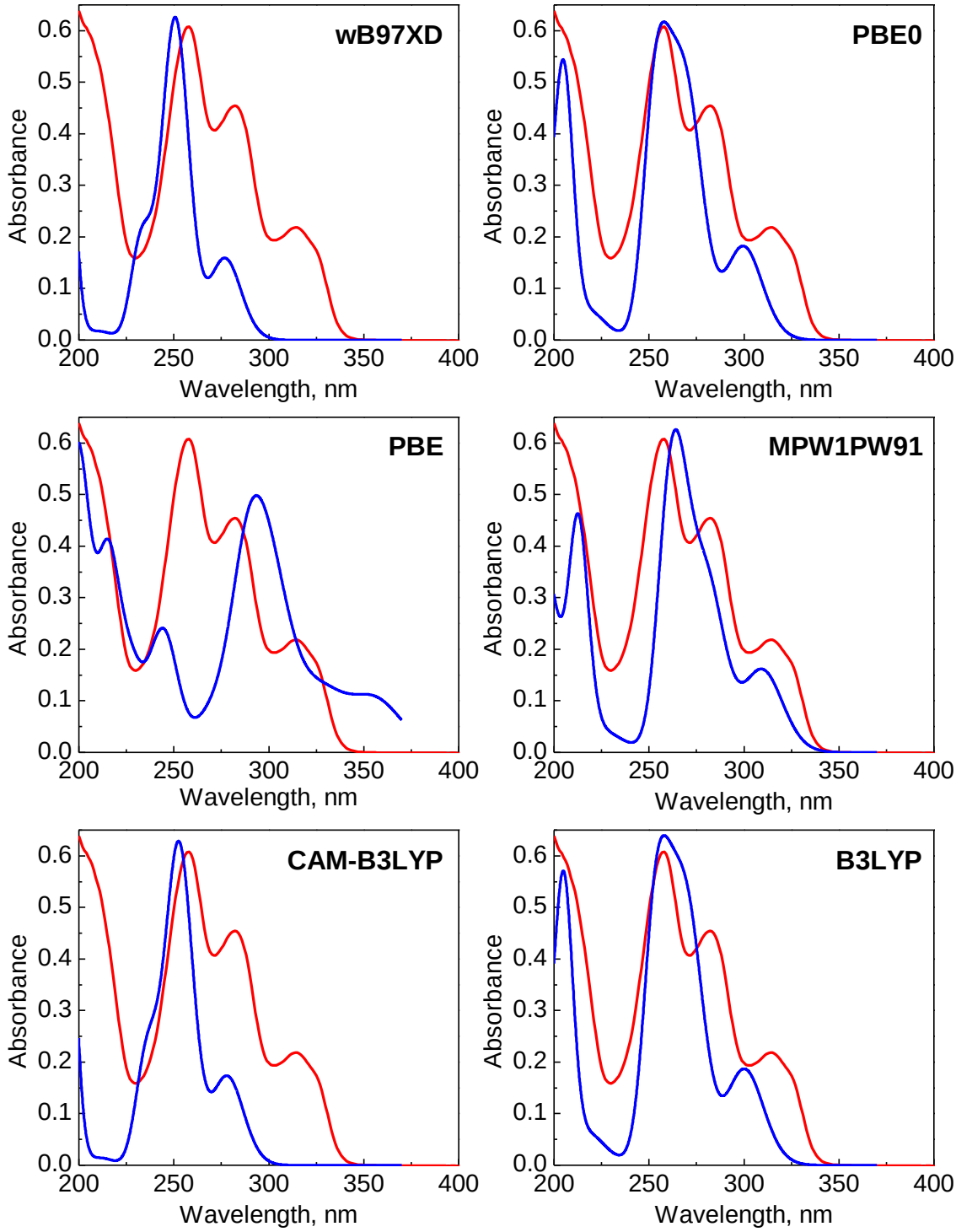

Fig. S18 The experimental (red) and calculated (blue) absorption spectra of L obtained using various functionals (both for the geometry optimization and for the spectrum calculation).

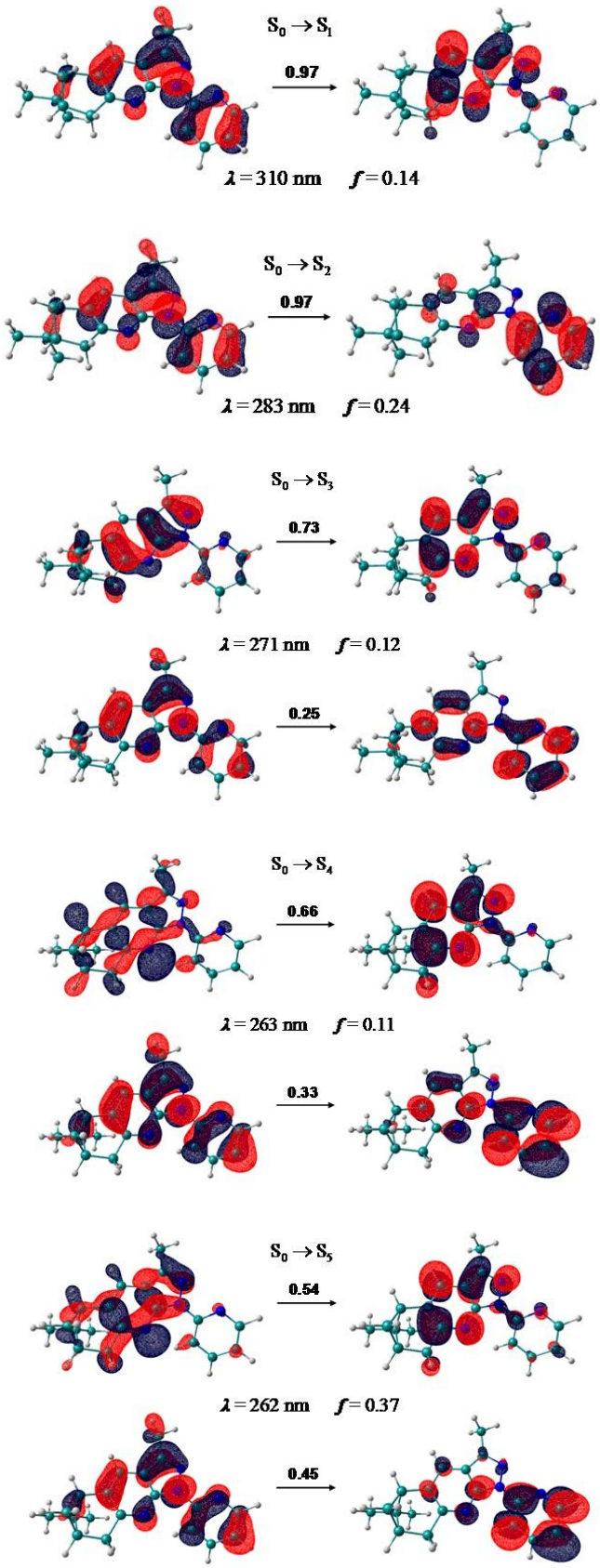

Fig. S19 The nature of the molecular orbitals of L involved in the first five transitions ($S_0 \rightarrow S_{1,2,3,4,5}$). The contribution of the corresponding transitions and the oscillator strengths are also indicated.

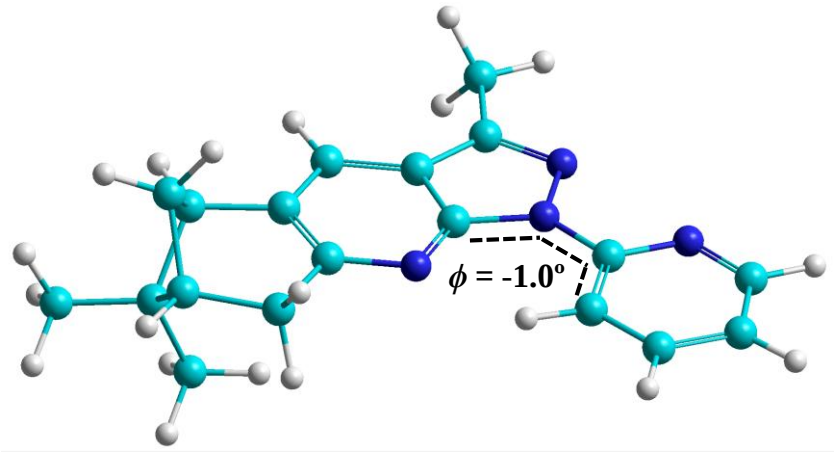

Fig. S20 Optimized structure of L in the S_1 excited state within the PCM model. The C−N−C−C torsion angle is the angle between the averaged planes of 5- and 6-membered rings.